

We have previously established a translatable MIA model using live viral infection in domestic swine. Inoculation at late gestation targets the initiation of the brain growth spurt, which begins in the last third of gestation and continues into the first several postnatal months (27, 28). The gestational window investigated here (E76 to E97) is primarily characterized by ongoing innervation and synaptogenesis and the initiation of myelination (29–32) and is ~2 to 5 wk past the peak of neurogenesis (at E60), when the percent of immature neurons is rapidly declining (33, 34). This timing corresponds to late prenatal neurodevelopmental stages of the human fetus (roughly 28 to 38 wk of human gestation) (35) and to the first 1 to 2 postnatal weeks in rodents (27, 34, 36, 37). Similarities between humans and pigs in brain anatomy, neurodevelopment, neurochemistry, and immunity (reviewed in refs. 29, 38, and 39) distinguish precocial swine from altricial rodents, making the pig a good model for human neurodevelopmental disorders. Data from our MIA pig model confirm the manifestation of altered behaviors in neonatal piglets (40). Fetal piglets exposed to MIA also have reduced neuronal density in the hippocampus and evidence of astrogliosis before birth (41). In the current study, we show that fetal porcine microglia are indeed globally altered during MIA. Furthermore, differential expression profiles between microglia of female versus male fetuses indicate sexual dimorphisms during healthy neurodevelopment, which are perturbed in response to prenatal insult.

Results

Maternal Porcine Reproductive and Respiratory Syndrome Virus Infection Causes Inflammatory Responses That Breach the Maternal-Fetal Interface. Pregnant gilts were inoculated with live porcine reproductive and respiratory syndrome virus (PRRSV) or sterile media during late gestation (gestational day [GD] 76) (study design is depicted in Fig. 1A). Circulating proinflammatory cytokines IL-6 and TNF α (Fig. 1B) were elevated in PRRSV-infected gilts compared to controls at both time points. Maternal infection resulted in transient increases in gilt body temperature (Fig. 1C) and a decrease in food intake (Fig. 1D). Gene expression analysis of endometrial tissue revealed an up-regulation of *IFNG*, *TNF*, *IL1B*, *CXCR3*, and *IL6* at 7 dpi and *IFNG*, *TNF*, and *CXCR3* at 21 dpi (Fig. 1E).

Litter size affected both fetal body weight and brain weight at both time points (*SI Appendix*, Table S1; litter characteristics in *SI Appendix*, Table S2). Body weights did not differ at either time point, but maternal infection resulted in decreased fetal brain weight ($P < 0.0001$; *SI Appendix*, Table S1) at 21 dpi; there was also a main effect of sex on brain weight at this time point, wherein female fetuses had lower brain weights compared to males ($P < 0.0001$, no maternal treatment \times sex interaction; *SI Appendix*, Table S1). All fetal groups were balanced for sex, and where applicable, this biological variable was included in statistical models due to the profound importance of sex in neuroimmunity (42); to provide a foundation for future studies, *SI Appendix* includes data separated by sex with sample sizes too small to include in the main text. At 7 dpi, *TNF* expression in placental tissue was elevated in MIA fetuses ($P < 0.05$) (Fig. 1F). At 21 dpi, *TNF* expression remained elevated in MIA placental tissue, with an additional increase in *IL1B* ($P < 0.01$) (Fig. 1F). Consistent with previous data (14), placental *IL6R* expression was unchanged between treatment groups; neurotrophin *BDNF* and cytokine *IL10* also did not differ (*SI Appendix*, Fig. S1). Circulating cytokines (TNF α , IL-10, IL-1 β , and IL-6) measured in amniotic fluids and fetal cord blood were below detection levels.

Fetal Microglia Transiently Alter Molecular Phenotype and Activity Following MIA. Primary microglia (CD11b⁺ CD45^{low}) isolated from fetuses at both 7 and 21 dpi were assessed using flow cytometry for expression of antigen-presenting and phagocytic markers MHCII and CD68. All primary microglia expressed

CD45 at low levels, distinguishing them from peripheral monocytes (representative scatter plots in *SI Appendix*, Fig. S2). At 7 dpi, primary microglia from MIA fetuses expressed more MHCII (Fig. 2A) but not CD68 (Fig. 2B) compared to controls; overall, percent of primary microglia expressing both markers (MHCII⁺CD68⁺) increased due to MIA (Fig. 2C). There was no effect of sex on MHCII or CD68 expression at 7 dpi. Isolated primary microglia were also assessed for phagocytic and chemotactic activity in vitro, with MIA cells displaying decreased phagocytosis (Fig. 2D) and chemotaxis (Fig. 2E) regardless of stimulation.

Microglia isolated from fetuses at 21 dpi still expressed more MHCII due to MIA (Fig. 2F), although CD68 expression (Fig. 2G) and coexpression of both markers (Fig. 2H) no longer differed between treatment groups. Males tended to have more MHCII⁺ CD68⁺ microglia compared to females, regardless of maternal treatment ($P = 0.10$) (*SI Appendix*, Fig. S3). The percent of microglial cells expressing CD68 decreased from 7 to 21 dpi ($P < 0.0001$; 7 dpi, $28.5 \pm 0.6\%$, $n = 79$; 21 dpi, $11.9 \pm 0.8\%$, $n = 97$). Microglia isolated at 21 dpi no longer differed in phagocytic activity due to MIA, although pretreatment with either LPS or poly I:C lowered phagocytosis (Fig. 2I). Chemotaxis remained reduced in microglia isolated from MIA fetuses at 21 dpi (Fig. 2J), although to a lesser extent compared to 7 dpi. Interestingly, gestational day, and not maternal viral infection, impacted production of TNF α by microglia in vitro, such that microglia isolated at GD 83 and treated with saline or LPS produced more TNF α compared to microglia isolated at GD 97; cells stimulated with poly I:C did not show this effect (*SI Appendix*, Fig. S4).

Maternal Viral Infection Alters Microglia-Enriched Genes. Using high-throughput qPCR, 47 target genes (*SI Appendix*, Table S3) involved in neurodevelopment, the microglia sensome, and inflammation, which are highly enriched in microglia (43), were examined to assess the response of fetal microglia to MIA at both 7 and 21 dpi. The microglia sensome describes a collection of transcripts encoding transmembrane receptors and proteins that sense endogenous and exogenous ligands (43); a subset of these genes was examined here. *IL17A*, which encodes cytokine IL-17a, and *CXCL2*, which encodes granulocyte chemoattractant protein chemokine (C-X-C motif) ligand 2, failed to amplify, leaving 45 total genes. In an attempt to parse out possible sex effects that may be present in our MIA model, and given the robustness of the high-throughput qPCR method, we designed this analysis as a 2 by 2 factorial to examine both MIA and sex effects (for both microglia and amygdala tissue). Interestingly, few genes were altered by MIA in microglia, and none by sex, at 7 dpi. MIA increased the expression of brain derived neurotrophic factor *BDNF*, chemokine receptor *CXCR2*, IFN induced *IFIT3*, atypical chemoattractant receptor *CCRL2*, Fc (IgE) receptor *FCER1G*, and *IL6* (Fig. 3); although microglia from MIA females demonstrated a higher expression of each of these genes, neither the main effect of sex nor the interaction between MIA and sex reached significance.

At 21 dpi, however, microglial expression of almost all 45 genes was altered due to the interaction between MIA and sex, rather than by MIA or sex alone (Fig. 3; means separations in *SI Appendix*, Table S4). Interestingly, *BDNF*, *CXCR2*, *IFIT3*, *CCRL2*, *FCER1G*, and *IL6* expression no longer differed across treatment groups as they had at 7 dpi but instead were impacted by sex alone, with the exception of *BDNF* and *IL6* ($P \leq 0.10$ for main effect of sex on *CXCR2* and for MIA by sex interaction on *FCER1G*). An overall pattern of increased gene expression in control females compared to control males was principally apparent, while this sexual dimorphism was not evident in MIA microglia (outside of the 6 aforementioned genes and *IL8*). This gene expression signature indicates disparate regulation by MIA as development progresses, causing a masking of the presumably normal sexual

variation occurring at this time point. Only 4 genes were impacted by MIA alone (crystallin beta B1 *CRYBB1*, transcription factor *EGR-1*, and proinflammatory cytokines *IFNG* and *TNF*), each with a significantly lower expression compared to controls.

A small subset of microglial genes of interest was also examined using standard qPCR (SI Appendix, Table S5; primer information in SI Appendix, Table S6). There were no differences in *IL6R* expression in microglia at 7 dpi, despite the increase in *IL6* at this time point; however, at 21 dpi, expression of *IL6R* was increased in MIA microglia (SI Appendix, Table S5). Expression of *STAT3* was not impacted at either time point. Interestingly, though the percent of MHCII⁺ primary microglia increased at both 7 and 21 dpi due to MIA, there were no significant impacts of MIA on *SLA-DR4* (MHCII) gene expression (SI Appendix, Table S5).

Microglia-Enriched Genes Are Altered in Fetal MIA Brain Tissue, Particularly in the Amygdala. The same set of microglia-enriched genes (SI Appendix, Table S3) were assessed in fetal amygdala tissue to investigate the impacts of MIA on brain tissue and specifically a region involved in social behavior. Previous data from our laboratory using this swine MIA model revealed that early postnatal sociability is decreased in MIA offspring compared to controls (40). We hypothesized that this gene set would be differentially regulated by MIA during fetal development and could contribute to changes in social behavior. *IFNG* and *IL1B* at both time points (and *TNF* at only 21 dpi) were excluded due to inconsistent amplification. At 7 dpi, only 4 genes were significantly impacted due to MIA alone (complement component *C5*, epigenetic regulator *DNMT1*, transmembrane adaptor *DAP12*

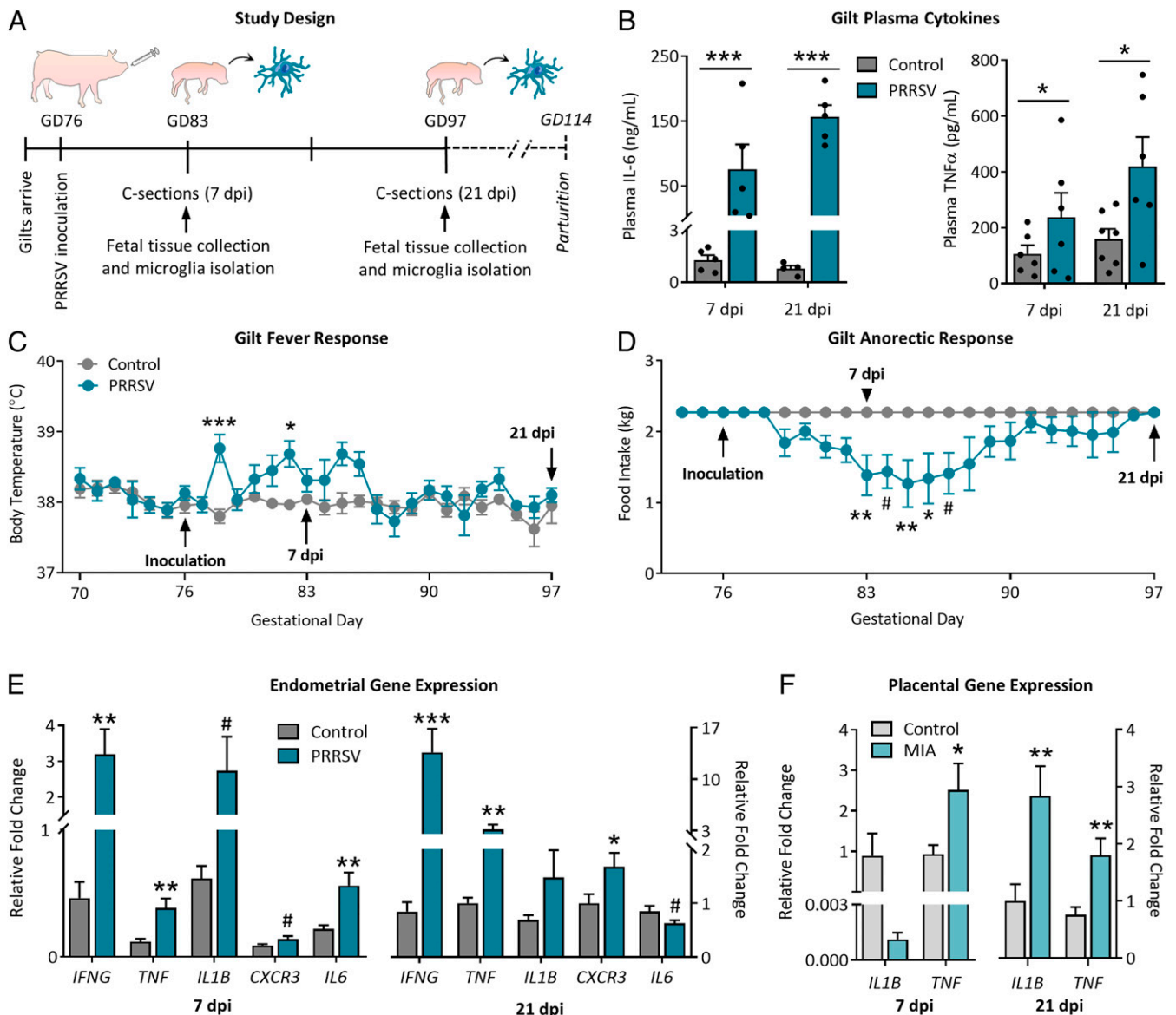


Fig. 1. PRRSV infection causes maternal inflammation and sickness responses. (A) Study design: Pregnant gilts were inoculated with PRRSV on GD 76, and cesarean sections were performed 7 and 21 dpi. (B) PRRSV-inoculated gilts had elevated plasma IL-6 and TNF α at 7 and 21 dpi (main effect of PRRSV, IL-6 = $P < 0.0001$, TNF α = $P < 0.05$). $n = 5$ to 7 per group per time point. PRRSV infection resulted in (C) increased body temperature (treatment \times time, $P < 0.0001$) and (D) decreased food intake (treatment \times time, $P < 0.0001$). GD 70 to 83, $n = 13$ to 14 per group; GD 83 to 97, $n = 6$ to 7 per group. Symbols indicate Bonferroni post hoc adjusted P values. (E) PRRSV infection resulted in an up-regulation of inflammatory genes in maternal endometrial tissue at both 7 and 21 dpi. $n = 5$ gilts per group per time point. (F) Maternal infection also resulted in an up-regulation of *TNF* and *IL1B* in fetal placental tissue. $n = 6$ to 11 fetuses per group per time point. *** $P < 0.001$, ** $P < 0.01$, * $P < 0.05$, and # $P < 0.10$; error bars are \pm SEM.

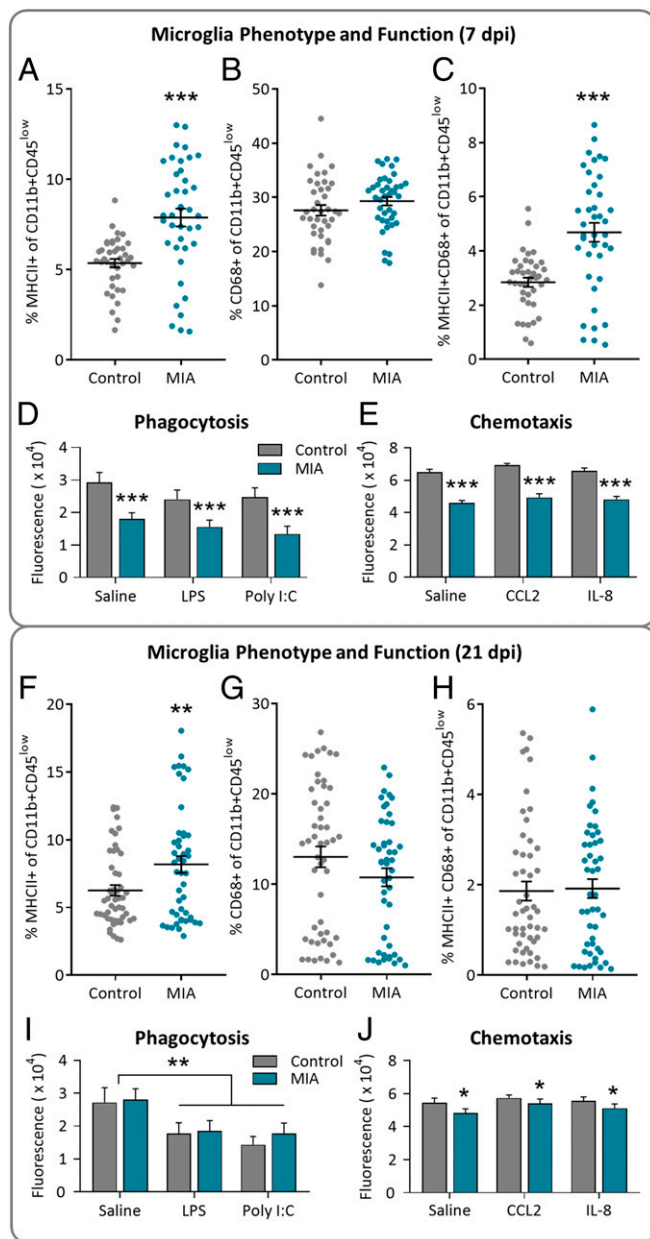


Fig. 2. Fetal microglia phenotype and function was altered by maternal infection. Maternal infection resulted in an increase in MHCII⁺ microglia and a reduction in microglia phagocytosis and chemotaxis. (A–E) 7 dpi and (F–J) 21 dpi. (A–E) Percentage of primary CD11b⁺CD45^{low} microglia expressing (A) MHCII, (B) CD68, or (C) both MHCII and CD68; $n = 4$ to 5 litters per group, $n = 39$ to 40 fetuses per group. MIA primary fetal microglia had (D) decreased phagocytic activity and (E) decreased chemotactic activity at 7 dpi. There was no effect of in vitro treatment, $n = 7$ to 16 fetuses per group; main effect of MIA, $***P < 0.0001$. (F–J) Percentage of primary microglia expressing (F) MHCII (main effect MIA, $**P < 0.01$), (G) CD68, or (H) both MHCII and CD68. $n = 5$ litters per group; $n = 47$ to 50 fetuses per group. MIA primary fetal microglia displayed phagocytic activity comparable to controls (I; main effect of in vitro treatment, $**P < 0.01$) but presented with reduced chemotactic activity (J; main effect of MIA, $*P < 0.05$; no effect of in vitro treatment) at 21 dpi. $n = 7$ to 16 fetuses per group; error bars are \pm SEM.

[*TYROBP*], and NF- κ B subunit *RELA*), with an interaction between MIA and sex on IFN γ receptor *IFNGR1* (Fig. 4; means separation in *SI Appendix, Table S7*). Nearly twice as many genes were impacted by sex alone, whereby females' expression was significantly higher compared to males, regardless of maternal

treatment. Expression of *TYROBP* and *RELA* was altered due to both MIA and sex (the interaction between MIA and sex did not reach significance), reflecting a much wider discrepancy between the sexes of the control group compared to MIA. Interestingly, sex no longer impacted gene expression at 21 dpi, with all alterations in expression arising only from the main effect of MIA (Fig. 4). An overall pattern of reduced expression in control fetuses compared to MIA, regardless of sex, was apparent in the amygdala at this point, with 15 genes reaching significance.

Whole fetal hippocampal and hypothalamic tissue was also examined for changes in inflammatory gene expression at both time points. At 7 dpi, there was no effect of MIA on gene expression in the hippocampus, while in the fetal hypothalamus, MIA caused a reduction in both *IL6* and IL-1 receptor antagonist (*IL1RA*) expression (*SI Appendix, Table S8*). No differences between groups were observed at 21 dpi (*SI Appendix, Table S9*).

Number and Morphology of Fetal Hippocampal Microglia Were Relatively Unchanged by MIA.

Previous data from our laboratory indicated that MIA reduces total neuron number in the fetal hippocampus, specifically in the dentate gyrus (41). We hypothesized that altered microglial density and activation in this region could contribute to this loss. To assess this possibility, microglia number and morphology were analyzed in the dentate gyrus and hilar regions of the fetal hippocampus through ionized calcium-binding adapter molecule 1 (Iba1) immunohistochemical staining. Representative images of fetal Iba1⁺ cell densities are presented in Fig. 5A; maternal infection did not impact total microglia number at either time point (Fig. 5B; results displaying sex are presented in *SI Appendix, Fig. S5A*). Gestational timing did not impact microglia number in the dentate gyrus and hilar region (Fig. 5B) ($P > 0.10$; GD 83, 346 ± 20 Iba1⁺ cells per square millimeter, $n = 17$; GD 97, 310 ± 18 Iba1⁺ cells per square millimeter, $n = 15$).

Although MIA did not significantly impact microglia number, a skewing of microglia toward a more cytotoxic phenotype might also contribute to a loss of neurons (1). As the persistent immune surveyors of the brain, microglia continuously shift through a spectrum of morphological states which closely align with the functions they are performing (44–46). More amoeboid cells (with retracted processes and enlarged cell bodies) often reflect more proinflammatory, reactive, and proliferative states and are the predominant morphology in the immature embryonic brain (1, 47, 48), whereas more mature cells take on a ramified phenotype (with elongated, branched processes and small cell bodies) and reflect a resolving and surveying state. Here microglia morphology was assessed by categorizing each cell into 1 of 4 phenotypes (depicted in Fig. 6A) based on the predominant morphologies observed in the embryonic mouse brain as maturation progresses (47). However, at 7 and 21 dpi, microglia morphologies in the dentate gyrus and hilar region did not significantly differ between treatment groups (*SI Appendix, Fig. S5 B and C*). As brain development progressed from GD 83 to GD 97, the total number of fetal microglia displaying thick, long processes decreased ($P < 0.05$; GD 83, 46 ± 6 Iba1⁺ cells per square millimeter, $n = 16$; GD 97, 25 ± 7 Iba1⁺ cells per square millimeter, $n = 15$); no other microglia morphologies were impacted by gestational timing within the dentate gyrus and hilus.

Microglial cell soma size, the morphological parameter which most closely correlates with increased Iba1- and CD68-dependent migration and phagocytosis (49, 50), was assessed as previously described (51). There was no effect of MIA on soma length, width, length-to-width ratio, or estimated area at either time point (*SI Appendix, Table S10*). However, microglia soma length, width, and estimated area increased as gestation progressed ($P < 0.01$, $P < 0.0001$, and $P < 0.0001$, respectively) (*SI Appendix, Table S11*), resulting in a decrease in length-to-width ratio from GD 83 to GD 97 ($P < 0.05$) (*SI Appendix, Table S11*).

MIA Alters Microglia Number, but Not Morphology, in the Fetal Amygdala. As piglets born to PRRSV-infected gilts demonstrate reduced social behavior during early life (40), we hypothesized that fetal microglia may be altered specifically in brain regions involved in social behavior, such as the amygdala. Indeed, examination of microglia number revealed a significant increase in Iba1⁺ cells per square millimeter in the amygdala of MIA fetuses at 7 dpi (Fig. 6B), although this did not persist to 21 dpi (results displaying sex are presented in *SI Appendix*, Fig. S6A). Advancement of gestational timing significantly increased the total number of microglia within the fetal amygdala ($P < 0.0001$; GD 83, 158 ± 15 Iba1⁺ cells per square millimeter; GD 97, 295 ± 11 Iba1⁺ cells per square millimeter) (representative images in *SI Appendix*, Fig. S6B). Despite these differences in total microglia number, microglia morphology within the amygdala did not differ due to maternal treatment at 7 dpi (Fig. 6C) or 21 dpi (Fig. 6D). However, in agreement with the increase in total microglia due to gestational timing, there was an increase in the number of amoeboid microglia, microglia with stout processes, and microglia with long, thick processes at GD 97 compared to GD 83 ($P < 0.001$) (*SI Appendix*, Fig. S6C); total microglia with thin,

ramified processes did not differ across gestation. Assessment of microglia soma size revealed no changes in length, width, length-to-width ratio, or estimated area at 7 dpi (*SI Appendix*, Table S12). Although soma length was decreased in microglia from MIA fetuses at 21 dpi ($P < 0.05$) (*SI Appendix*, Table S12), no other parameter of soma size was impacted by MIA.

Notably, microglia characteristics differed between the 2 discrete brain regions of the hippocampus and amygdala, regardless of maternal treatment. There was a higher density of Iba1⁺ cells in the dentate gyrus/hilar region compared to the amygdala at 7 dpi, but this normalized by 21 dpi (*SI Appendix*, Fig. S7A and C) due to the increase in cell density within the amygdala between GD83 and GD97. Additionally, the percent of cells categorized into each of the 4 morphologies differed across all categories at 7 dpi (*SI Appendix*, Fig. S7B); this continued into 21 dpi, where percentages differed in all but 1 morphological category (*SI Appendix*, Fig. S7D). Cell soma measurements differed accordingly between the regions, such that microglia in the amygdala had larger somas (length, width, and estimated area) compared to microglia in the hippocampus at both time points (*SI Appendix*, Fig. S8).

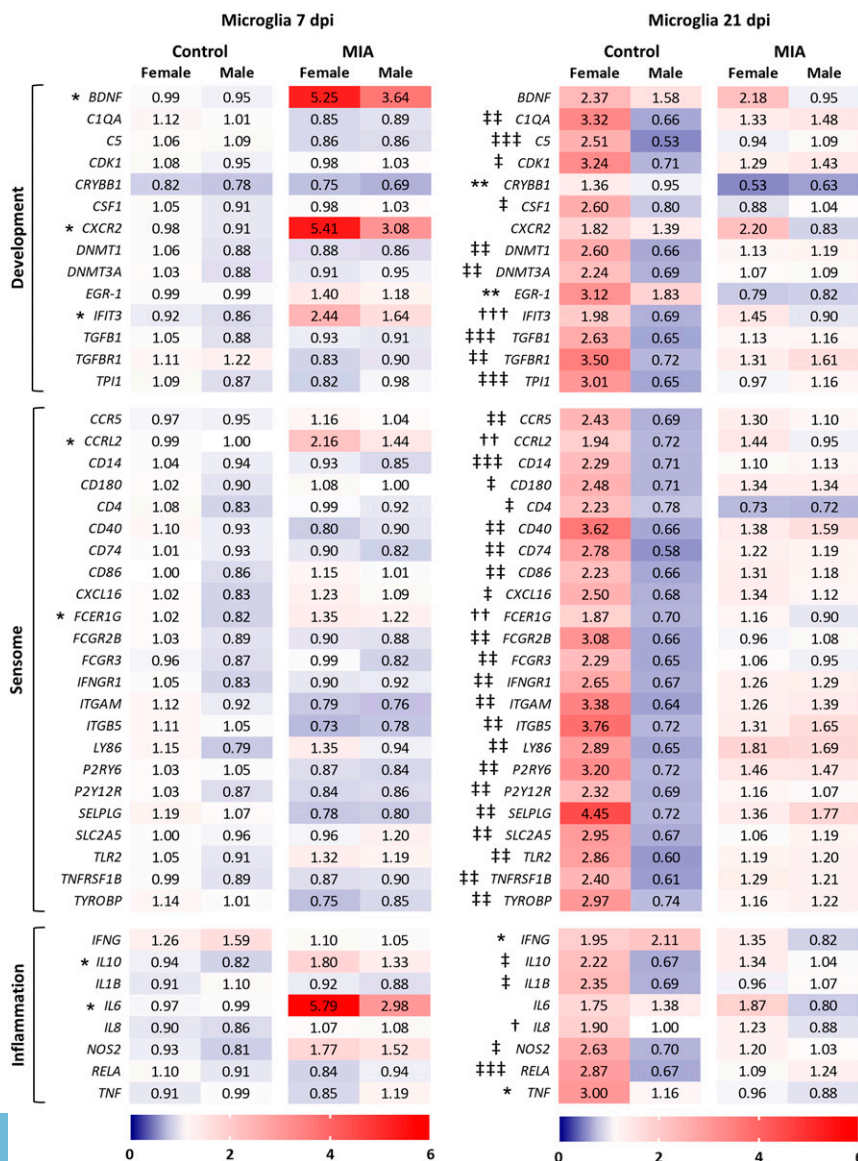


Fig. 3. Maternal viral infection alters microglia-enriched genes. Gene expression assessed in primary fetal microglia at (Left) 7 and (Right) 21 dpi. Target genes are highly enriched in microglia and involved in neurodevelopment, the microglia sensesome, and inflammation. Results are expressed as average fold-change; $n = 10$ to 15 per sex per group per time point; an asterisk (*) indicates main effect of MIA, a dagger (†) indicates main effect of sex, and a double cross (‡) indicates MIA \times sex interaction; and 3 symbols = $P < 0.001$, 2 symbols = $P < 0.01$, and 1 symbol = $P < 0.05$.

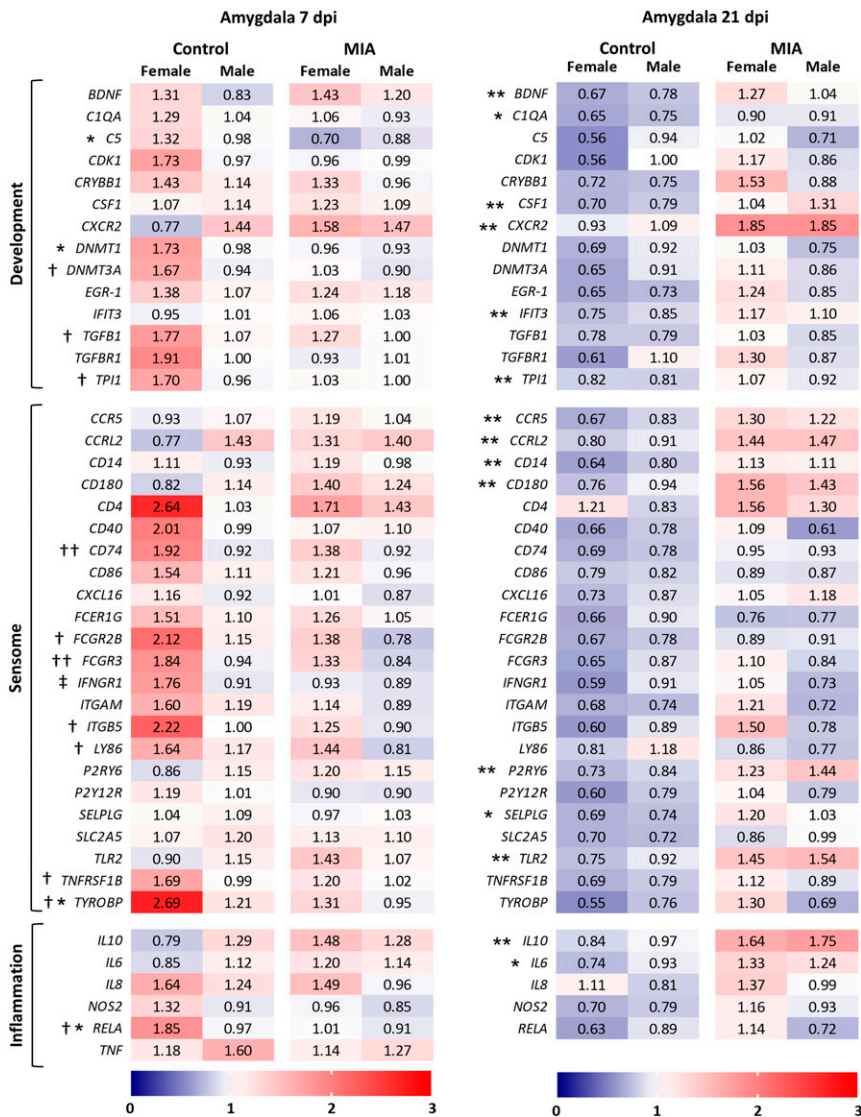


Fig. 4. Microglia-enriched genes are altered in the fetal amygdala. Gene expression assessed in whole amygdala tissue at 7 and 21 dpi. Results are expressed as average fold-change; $n = 10$ to 14 per sex per group per time point; an asterisk (*) indicates main effect of MIA, a dagger (†) indicates main effect of sex, and a double cross (‡) indicates MIA \times sex interaction; and 3 symbols = $P < 0.001$, 2 symbols = $P < 0.01$, and 1 symbol = $P < 0.05$.

Discussion

In the current study, we demonstrate that fetal microglia from a gyrencephalic species are globally altered by maternal viral infection. As we have reported previously, MIA in swine reduces overall fetal brain weight but not body weight (41), emphasizing the concentrated impact of MIA on brain development emerging within 3 wk post-maternal viral inoculation. Inflammation at the maternal–fetal interface, a likely pathway through which maternal cytokines signal to the fetal brain (14, 15, 52), was present even after maternal symptoms resolved. Decreased phagocytic and

chemotactic capacity and increased expression of MHCII in fetal microglia during peak maternal infection were normalizing by 21 dpi. However, widespread modifications in expression of microglial-enriched genes endured longer, indicating persistent differential regulation of processes important for neurodevelopment and sensing of endogenous signals and danger molecules. Microglia density was increased at 7 dpi specifically in the fetal amygdala, a brain region integral to the control of social behaviors; despite stabilized microglia numbers at 21 dpi, this transient fluctuation may be sufficient to alter neurodevelopment. Our data also indicate

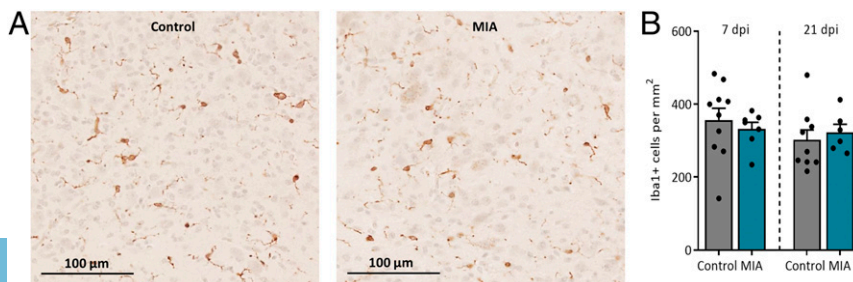


Fig. 5. Maternal infection does not impact fetal microglia density in the hippocampus. (A) Representative images of Iba1⁺ cell densities of control and MIA fetuses within the dentate gyrus/hilar region of the hippocampus at 20 \times magnification. (Scale bar, 100 μ m.) (B) Neither maternal infection nor gestational time impacted microglia density. Error bars are \pm SEM; $n = 6$ to 10 fetuses per group.

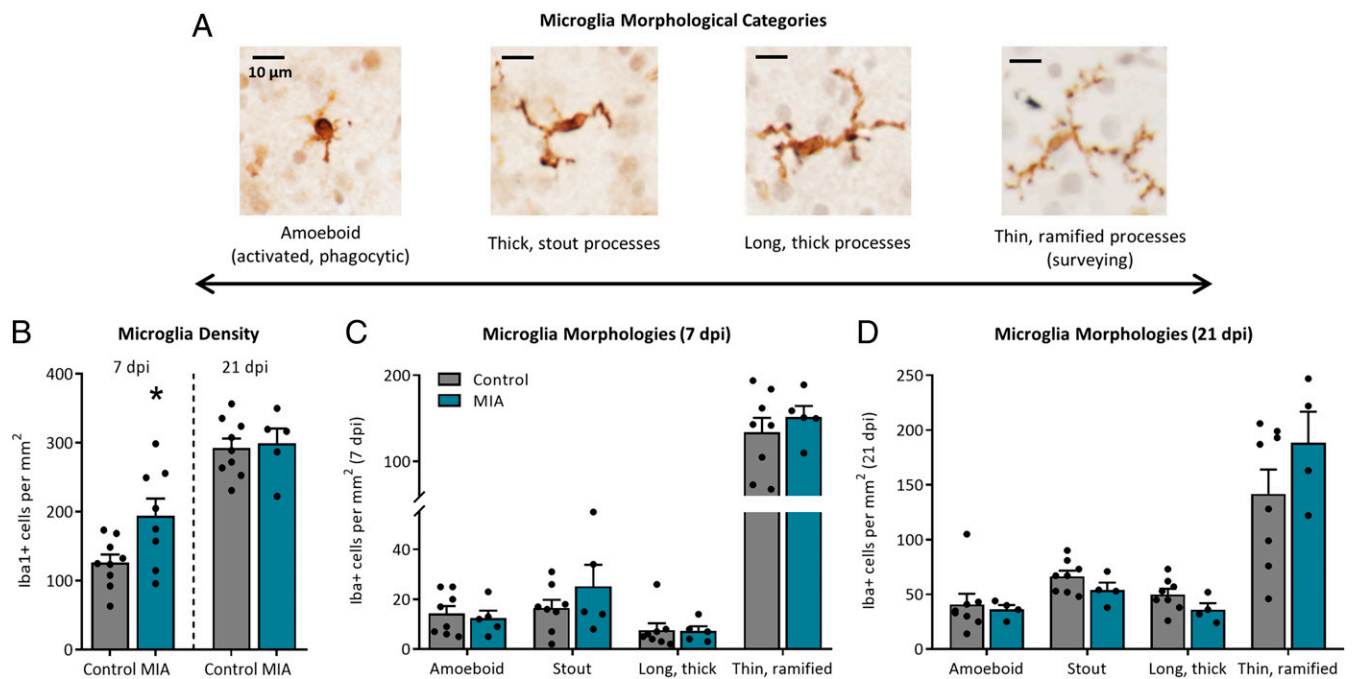


Fig. 6. Maternal infection transiently impacts microglia density but not morphology in the fetal amygdala. (A) Representative images of 4 microglia morphologies within the fetal pig brain at 40× magnification. (Scale bar, 10 μm.) (B) At 7 dpi, MIA fetuses displayed more microglia in the amygdala compared to controls ($*P < 0.05$) but no longer differed at 21 dpi. At (C) 7 and (D) 21 dpi, microglia morphology in the amygdala did not differ between treatment groups, and most microglia displayed ramified morphology. Error bars are \pm SEM; $n = 5$ to 9 fetuses per group.

that certain microglial characteristics, such as production of TNF α and cell morphology and density, are impacted by gestational timing, coinciding with colonization and maturation patterns of newborn microglia (53, 54). Widespread sexual dimorphisms among microglial gene expression patterns align with current concepts in the field (42, 55, 56).

Maternal cytokines, particularly IL-6 (13–15) and IL-17a (16–18), have been implicated as the chief mediators of altered neurodevelopment and behavior in MIA. Here we show that pregnant gilts infected with PRRSV have increased levels of IL-6 and TNF α in circulation and that these elevated levels persist even after sickness symptoms have resolved. Although swine do have T_H17 cells that produce IL-17a (57, 58), plasma IL-17a was not impacted by PRRSV infection at the times sampled, suggesting that translation of maternal inflammatory signaling to the fetal brain may not include IL-17a in our model (59). Additionally, although fetal tissues were examined for *IL17A* mRNA, there was poor amplification across all tissues; *IL17R* mRNA was not measured. Nonetheless, increases in IL-6 and TNF α were mirrored in increased gene expression of both cytokines in endometrial tissue at 7 dpi. Interestingly, *CXCR3*, a chemokine receptor expressed on T_H1 cells (60), was increased at 21 dpi, suggesting effector T cell infiltration. This aligns with the 3- and 15-fold tissue-specific increase in *IFNG* at 7 and 21 dpi, respectively, as IFN γ not only induces *CXCR3* ligands (60) and directs T_H1 cell differentiation but also is produced by T_H1 cells; these cells may also contribute to the 3-fold increase in *TNF* expression at 21 dpi.

Previous studies have found changes in placental gene expression (52, 61), including neurotrophic genes (62, 63), following MIA. In the porcine placenta, maternal infection caused increases in proinflammatory cytokines *TNF* and *IL1B*. Although placental neurotrophin production may correlate to production in the developing brain during MIA (62, 63), this was not overtly true here. Microglial expression of *BDNF*, which promotes new synapse formation (64), was substantially increased by MIA at 7 dpi and may be a neuroprotective response (65, 66); this did not persist to

21 dpi. However, microglial contributions to total brain BDNF concentrations are minimal (67), and likely region-specific, which was evidenced by the delayed induction of *BDNF* expression in whole amygdala tissue. Unlike humans and rodents, swine have a noninvasive epitheliochorial placenta, where placental trophoblasts do not directly contact maternal blood. This difference in tissue structure at the maternal–fetal interface may delay inflammatory signaling from the maternal endometrium to fetal tissues, which would explain why few changes in placental gene expression were evident at 7 dpi, even though inflammatory genes were increased in maternal tissues at this time. Contrary to evidence presented in rodent models (14, 15), *IL6* expression was not up-regulated in the porcine placenta at either time point; however, it is important to note that placentas from rodent studies were assessed within hours of MIA induction, which does not exactly align with the 7 and 21 dpi time points presented here. Thus, signaling of IL-6 through the placenta cannot be ruled out in our model.

As with the periphery, MIA-induced immune changes were also evident in fetal porcine microglia, specifically in function and phenotype. Flow cytometric analysis of fetal microglia showed that few cells displayed surface MHCII (major histocompatibility complex class II); nonetheless, MIA caused a 2 to 3% increase in this antigen-presenting molecule at both time points. As MHCII is up-regulated during pathological CNS states (68, 69), as well as during postnatal PRRSV infection (51, 70), this could suggest that fetal microglia transiently shift to a more reactive state during maternal PRRSV infection. Given that IFN γ is a primary driver of MHCII mobilization, a reduction in MIA microglia *IFNG* expression at 21 dpi (as well as *TNF*) could suggest a compensatory shift toward a less reactive and more resolving state. Further support for this may be reflected in the disparate regulation of *TGFBR1* and *TGFB1* expression at this same time point. Activation of the TGF- β receptor, and production of TGF- β protein, is integral for resolving neuroinflammation (71), and for proper microglia development (72). During embryonic development, TGF- β signaling is vital for microglial cell survival (72) and helps

maintain a more quiescent or homeostatic phenotype after cell maturation (73, 74). While control microglia display sexually dimorphic expression of both of these genes, male and female MIA microglia appear to be up- and down-regulating expression, respectively, such that expression levels between the sexes normalize, indicating that mechanisms in microglial mRNA regulation, at least at this time point, are sex dependent.

On the contrary, the percent of microglia positive for CD68 was not impacted by MIA. CD68 is expressed both on lysosomes and the plasma membrane and is used as an indicator of active phagocytosis (75); here membrane, but not lysosomal, expression was measured. Functional *in vitro* assessment of microglial phagocytosis, however, indicated reduced phagocytic uptake of *Escherichia coli* compared to control microglia at 7 dpi, although this normalized by 21 dpi. This is consistent with data from Mattei et al. (76), who showed a similar reduction of adult microglial phagocytosis, along with disrupted transcription of molecules that are involved in phagocytic processes. Our data suggest that a comparable phenotype may be induced by MIA in gyrencephalic species, indicating that reduced microglial phagocytosis could be a primary route by which MIA impacts both fetal and adult brain function, although the exact consequences of this have yet to be elucidated.

This is in contrast to rodent data suggesting that MIA increases prenatal microglial phagocytosis, leading to a reduction in the neuroprogenitor pool (1); however, direct phagocytic capacity of embryonic rodent microglia was either not investigated or not reported by these authors. It is possible that microglial phagocytosis could be acutely increased and then reduced by 21 dpi, although further research is needed to parse this out. A diminished neuroprogenitor pool could be in agreement with the reduction in MIA fetal brain weight. However, inhibition or ablation of microglia (i.e., removal of trophic support) can also induce neuron death or inhibit neurogenesis and oligodendrogenesis (2, 77, 78). Microglia also promote astrocytic differentiation, in part through production of IL-6 and leukemia inhibitory factor (LIF) (79), and nitric oxide (NO) by way of NOS2 (80). We have previously shown that MIA in swine results in a reduction in estimated neuron density and increased astrocyte density in the hippocampus evident several days before birth, with no differences in cell proliferation (41). Thus, the persistent reduction in *in vitro* chemotactic capacity of MIA fetal microglia when stimulated with IL-8 and CCL2 is noteworthy. Microglial chemotaxis is controlled by binding of chemokines to their cell surface receptors, aiding in microglial cell migration throughout developing brain regions (81). Inhibiting microglial chemotactic motility during murine neocortical development impedes neural progenitor differentiation (81), replicating what is observed during microglial depletion (78). Thus, it is possible that it is not increased microglial phagocytosis but reduced chemotaxis that ultimately results in smaller brain weights through diminished trophic support. Perhaps as a compensatory response, expression of *CXCR2*, the beta receptor for IL-8, was acutely up-regulated in MIA microglia at 7 dpi, especially in females; while MIA no longer had an effect at 21 dpi, this sexually dimorphic expression tended to persist. Furthermore, *in vitro* evidence suggests that IL-6 production by microglia may suppress neurogenesis in favor of astrogenesis (79); thus, the increased expression of microglial *IL6* at 7 dpi may be contributing to the increased GFAP staining and gene expression previously observed in our MIA model (41).

Notable among the genes dysregulated by MIA in microglia was a down-regulation of crystallin beta B1 (*CRYBB1*), which was one of the few genes not impacted by sex at 21 dpi. Crystallin proteins, including *CRYBB1*, are enriched in microglial populations (22, 43) and play a role in promoting immunoregulatory and neuroprotective phenotypes (82–84). Down-regulation in our model is contrary to previous data demonstrating acute induction of fetal brain crystallin expression in rodents using

3 different models of MIA (82). Dysregulation of *CRYBB1* has been linked to schizophrenia (85), and down-regulation in the medial prefrontal cortex can alleviate anxiety-like behavior in mice (86). Further research is needed to understand if dysregulated *CRYBB1* expression persists beyond the prenatal period and how this may affect microglial immunoregulatory phenotype and postnatal behaviors. Disparate regulation of microglial and amygdalar *CSF1* expression, which encodes macrophage colony stimulating factor, was also present at 21 dpi. CSF-1 receptor (CSF-1R), expressed constitutively on microglia, is essential for microglial colonization and proliferation during development and for proliferation and survival throughout the lifespan (53, 87). CSF-1 is especially enriched in microglia during neurodevelopment (22); thus, disrupted expression of *CSF1* at 21 dpi and of cell cycle-associated gene transcription factor early growth response protein 1 (*EGR-1* (22)) in MIA microglia could suggest a decline in autocrine signaling and cell proliferation. This could be a compensatory response to the increased density of microglia in the amygdala during peak maternal infection, a disparity which resolved by 21 dpi.

To date, the overproduction of cytokines in the MIA brain by microglia (1, 11, 12, 22) is thought to be a major contributor to altered neurodevelopment. Expression of proinflammatory cytokines (such as IFN γ , IL-1 β , IL-6, and TNF α) by microglia during healthy neurodevelopment is necessary for enhancing neurogenesis, oligodendrogenesis, and astrocytic differentiation (77, 79), and thus, a disruption in the production and release of these cytokines could alter brain development trajectories. Here microglial *IL6* expression acutely increased several fold, consistent with murine MIA studies emphasizing the specific involvement of IL6 in the fetal brain (13, 14). However, this appears to be cytokine specific as there was only a concurrent increase in *IL10* (and, although the effect of MIA did not quite reach significance, *NOS2*), while all other immune genes remained unchanged. Two weeks later, however, expression of *IL10*, *IL1B*, *NOS2*, and *RELA* was dysregulated, punctuated by a reduction in *IFNG* and *TNF*, an up-regulation of *IL6R*, and *IL6* expression that had normalized. In most MIA rodent studies, embryonic microglia are investigated at a single time point (1, 11, 12, 22) and not in the period after the maternal inflammatory response has resolved; the addition of the 3-wk postinoculation time point here, therefore, provides valuable information regarding which fetal responses resolve within this time and which persist. Notably, a delayed increase in the expression of *IL10* and *IL6* in 21 dpi MIA amygdala tissue emphasizes that cytokine production is not equivalent between microglial cells and whole brain tissue. Furthermore, discrete brain regions exhibited contrasting cytokine gene expression profiles, as *IL6* and *IL1RA* were reduced in the hypothalamus, while the hippocampus appeared relatively resilient in comparison.

Peripheral monocytes, which also express CD11b and are known to infiltrate the rodent brain during healthy neonatal development (87), could be contributing to these contrasting gene expression profiles. Although the genes examined here are specifically enriched in microglia, most are also expressed by macrophages in the periphery (43). While exploration of the subtypes and functions of hematopoietically derived resident CNS myeloid cells has recently begun (88), and there is some evidence that peripheral monocytes may impact early neurodevelopment (89), the roles of these different cell types are not well defined in the context of MIA and were not investigated here. However, nonmyeloid cell types within the brain, particularly neurons and astrocytes, could also be driving aspects of neurodevelopment in this context. For example, neuronal overexpression of chemokine receptor CCR5 has recently been implicated as a potent suppressor of synaptic plasticity and learning and memory in adult mice (90); here *CCR5* (along with several other chemokine receptors) was up-regulated in the MIA amygdala, and although further studies would be needed, this could have consequences for prenatal brain development as well. We

have also previously shown that maternal viral infection causes astrogliosis in prenatal swine (41); astrocytes are potent mediators of synaptic plasticity (91) and pruning (92, 93) and signal closely with microglia. It is possible that the prenatal microglial perturbations observed here augment astrogenesis or that these signals prime astrocytes, as astrocyte immunomodulation, and transformation into the reactive A1 phenotype, is dependent upon proinflammatory signals released by microglia (94, 95). These cells have also been implicated in MIA outside of our model (96, 97), and the potential for altered prenatal astrocyte activity in this context presents an important area for future research.

Separate from the impacts of maternal infection on microglial function and phenotype was a clear impact of gestational timing, likely indicative of a maturation of cells and circuits as development progressed. Indeed, the timing of maternal infection is a critical variable in predicting the risk of neurodevelopmental alterations (25, 98). Here *in vitro* microglial production of TNF α , at baseline and in response to LPS, was reduced as gestation advanced. Surface CD68 expression also diminished from GD 83 to GD 97. This aligns with the phenotypes of embryonic rodent and nonhuman primate microglia that are primarily amoeboid and phagocytic during development (1) but shift to a more ramified state as they mature, down-regulating classical inflammatory markers (53, 77). Thus, our data indicate that surface CD68 expression and *in vitro* production of TNF α may be good markers for microglial cell maturation during brain development. Microglia morphologies and soma size also evolved across the span of 3 gestational weeks, and these changes varied between the discrete amygdalar and hippocampal regions. This is consistent with gene profiling studies on rodent microglia, which describe distinct transcriptional and phenotypic profiles dependent on brain region (22, 43, 99, 100).

Overall, our data demonstrate that chemotactic and phagocytic functions of porcine fetal microglia are distinctly altered in response to late-gestation MIA, which corresponds to global changes in gene expression patterns and an acute increase in microglial cell density in the amygdala. Importantly, these changes appeared to be transient as almost all metrics of microglia function and phenotype progressed toward resolution by 21 dpi. However, lingering effects of MIA on gene expression patterns and on overall brain weight suggest that altered microglial func-

tion has prolonged impacts on neurodevelopment and subsequent postnatal social behaviors (40). This study demonstrates that fetal microglia in a gyrencephalic species are globally altered by MIA and sex, emphasizing that these cells likely play an important role in the development and sexual dimorphisms of neuropsychiatric disorders in humans.

Materials and Methods

Detailed materials and methods are described in *SI Appendix*.

Animals. Pregnant Large White/Landrace gilts were maintained as previously described (40, 41). All gilts were littermate pairs; 1 gilt from each pair was inoculated intranasal with 5 mL of 1×10^5 TCID₅₀ of live PRRSV (P-129-BV strain, obtained from Purdue University) at GD 76; the alternate littermate received sterile DMEM. Half the gilts were euthanized at GD 83 ± 1 d and half at GD 97 ± 1 d; cesarean sections were performed as previously described (41). All animal husbandry and experimentation were approved by the University of Illinois Institutional Animal Care and Use Committee.

Microglial Cell Isolation and Treatments. CD11b⁺ microglia were isolated as previously described (40). Cells from each fetus were split in half: one half for flow cytometric analyses and the other half for RNA isolation. Flow cytometric procedures were carried out as previously described (40). Microglia reserved for *in vitro* assays were incubated with LPS (1 ng/mL media), poly I:C (1 μ g/mL media), or sterile *d*-PBS for 4 h. Phagocytic and chemotactic activity was assessed as previously described (51).

High-Throughput qPCR Using the Fluidigm Amplification System. Quantitative PCR analysis was performed using the Biomark HD Fluidigm high-throughput amplification system and analyzed using the Biomark and EP1 Real-Time PCR Analysis Software. Delta delta Ct calculations were used to obtain fold-change of target genes compared to housekeeping control *RPL19*.

Iba1 Immunohistochemistry. Coronal slices were stained with anti-Iba1 rabbit primary antibody at 1:500 dilution and goat anti-rabbit IgG secondary antibody at 1:5,000 dilution. Signal was amplified using Vector ABC kit PK4000, and color was developed using 3,3'-Diaminobenzidine tetrahydrochloride (DAB) tablets.

ACKNOWLEDGMENTS. We thank Dr. William Van Alstine for providing porcine reproductive and respiratory syndrome virus. Funding was provided by the National Institutes of Health Grant HD069899.

- C. L. Cunningham, V. Martínez-Cerdeño, S. C. Noctor, Microglia regulate the number of neural precursor cells in the developing cerebral cortex. *J. Neurosci.* **33**, 4216–4233 (2013).
- M. Ueno *et al.*, Layer V cortical neurons require microglial support for survival during postnatal development. *Nat. Neurosci.* **16**, 543–551 (2013).
- P. Squarzoni *et al.*, Microglia modulate wiring of the embryonic forebrain. *Cell Rep.* **8**, 1271–1279 (2014).
- A. Sierra *et al.*, Microglia shape adult hippocampal neurogenesis through apoptosis-coupled phagocytosis. *Cell Stem Cell* **7**, 483–495 (2010).
- R. C. Paolicelli *et al.*, Synaptic pruning by microglia is necessary for normal brain development. *Science* **333**, 1456–1458 (2011).
- H. J. Kim *et al.*, Deficient autophagy in microglia impairs synaptic pruning and causes social behavioral defects. *Mol. Psychiatry* **22**, 1576–1584 (2017).
- Y. Zhan *et al.*, Deficient neuron-microglia signaling results in impaired functional brain connectivity and social behavior. *Nat. Neurosci.* **17**, 400–406 (2014).
- H. O. Atladóttir *et al.*, Maternal infection requiring hospitalization during pregnancy and autism spectrum disorders. *J. Autism Dev. Disord.* **40**, 1423–1430 (2010).
- S. Patel *et al.*, Social impairments in autism spectrum disorder are related to maternal immune history profile. *Mol. Psychiatry* **23**, 1794–1797 (2018).
- B. J. S. Al-Haddad *et al.*, Long-term risk of neuropsychiatric disease after exposure to infection in utero. *JAMA Psychiatry* **76**, 594–602 (2019).
- W. Schaafsma *et al.*, Maternal inflammation induces immune activation of fetal microglia and leads to disrupted microglia immune responses, behavior, and learning performance in adulthood. *Neurobiol. Dis.* **106**, 291–300 (2017).
- L. Pratt, L. Ni, N. M. Ponzio, G. M. Jonakait, Maternal inflammation promotes fetal microglial activation and increased cholinergic expression in the fetal basal forebrain: Role of interleukin-6. *Pediatr. Res.* **74**, 393–401 (2013).
- S. E. Smith, J. Li, K. Garbett, K. Mirnic, P. H. Patterson, Maternal immune activation alters fetal brain development through interleukin-6. *J. Neurosci.* **27**, 10695–10702 (2007).
- W. L. Wu, E. Y. Hsiao, Z. Yan, S. K. Mazmanian, P. H. Patterson, The placental interleukin-6 signaling controls fetal brain development and behavior. *Brain Behav. Immun.* **62**, 11–23 (2017).
- E. Y. Hsiao, P. H. Patterson, Activation of the maternal immune system induces endocrine changes in the placenta via IL-6. *Brain Behav. Immun.* **25**, 604–615 (2011).
- G. B. Choi *et al.*, The maternal interleukin-17a pathway in mice promotes autism-like phenotypes in offspring. *Science* **351**, 933–939 (2016).
- S. Kim *et al.*, Maternal gut bacteria promote neurodevelopmental abnormalities in mouse offspring. *Nature* **549**, 528–532 (2017).
- Y. Shin Yim *et al.*, Reversing behavioural abnormalities in mice exposed to maternal inflammation. *Nature* **549**, 482–487 (2017).
- S. Missault *et al.*, The risk for behavioural deficits is determined by the maternal immune response to prenatal immune challenge in a neurodevelopmental model. *Brain Behav. Immun.* **42**, 138–146 (2014).
- N. V. Malkova, C. Z. Yu, E. Y. Hsiao, M. J. Moore, P. H. Patterson, Maternal immune activation yields offspring displaying mouse versions of the three core symptoms of autism. *Brain Behav. Immun.* **26**, 607–616 (2012).
- M. D. Bauman *et al.*, Activation of the maternal immune system during pregnancy alters behavioral development of rhesus monkey offspring. *Biol. Psychiatry* **75**, 332–341 (2014).
- O. Matcovitch-Natan *et al.*, Microglia development follows a stepwise program to regulate brain homeostasis. *Science* **353**, aad8670 (2016).
- S. Smolders *et al.*, Maternal immune activation evoked by polyinosinic:polycytidylic acid does not evoke microglial cell activation in the embryo. *Front. Cell. Neurosci.* **9**, 301 (2015).
- D. Arsenault, I. St-Amour, G. Cisbani, L. S. Rousseau, F. Cichetti, The different effects of LPS and poly I:C prenatal immune challenges on the behavior, development and inflammatory responses in pregnant mice and their offspring. *Brain Behav. Immun.* **38**, 77–90 (2014).
- A. C. Kentner *et al.*, Maternal immune activation: Reporting guidelines to improve the rigor, reproducibility, and transparency of the model. *Neuropsychopharmacology* **44**, 245–258 (2019).
- S. Smolders, T. Notter, S. M. T. Smolders, J. M. Rigo, B. Bröne, Controversies and prospects about microglia in maternal immune activation models for neurodevelopmental disorders. *Brain Behav. Immun.* **73**, 51–65 (2018).

27. J. Dobbing, J. Sands, Comparative aspects of the brain growth spurt. *Early Hum. Dev.* **3**, 79–83 (1979).
28. M. S. Conrad, R. N. Dilger, R. W. Johnson, Brain growth of the domestic pig (*Sus scrofa*) from 2 to 24 weeks of age: A longitudinal MRI study. *Dev. Neurosci.* **34**, 291–298 (2012).
29. M. S. Conrad, R. W. Johnson, The domestic piglet: An important model for investigating the neurodevelopmental consequences of early life insults. *Annu. Rev. Anim. Biosci.* **3**, 245–264 (2015).
30. W. Qi *et al.*, Diffusion tensor MR imaging characteristics of cerebral white matter development in fetal pigs. *BMC Med. Imaging* **17**, 50 (2017).
31. J. W. Dickerson, J. Dobbing, Prenatal and postnatal growth and development of the central nervous system of the pig. *Proc. R. Soc. Lond. B Biol. Sci.* **166**, 384–395 (1967).
32. W. G. Pond *et al.*, Perinatal ontogeny of brain growth in the domestic pig. *Proc. Soc. Exp. Biol. Med.* **223**, 102–108 (2000).
33. K. B. Nielsen *et al.*, Reelin expression during embryonic development of the pig brain. *BMC Neurosci.* **11**, 75 (2010).
34. L. Ernst *et al.*, Fast prenatal development of the NPY neuron system in the neocortex of the European wild boar, *Sus scrofa*. *Brain Struct. Funct.* **223**, 3855–3873 (2018).
35. S. L. Andersen, Trajectories of brain development: Point of vulnerability or window of opportunity? *Neurosci. Biobehav. Rev.* **27**, 3–18 (2003).
36. E. Calabrese, A. Badea, C. Watson, G. A. Johnson, A quantitative magnetic resonance histology atlas of postnatal rat brain development with regional estimates of growth and variability. *NeuroImage* **71**, 196–206 (2013).
37. B. D. Semple, K. Blomgren, K. Gimlin, D. M. Ferriero, L. J. Noble-Haeusslein, Brain development in rodents and humans: Identifying benchmarks of maturation and vulnerability to injury across species. *Prog. Neurobiol.* **106–107**, 1–16 (2013).
38. N. M. Lind *et al.*, The use of pigs in neuroscience: Modeling brain disorders. *Neurosci. Biobehav. Rev.* **31**, 728–751 (2007).
39. K. H. Mair *et al.*, The porcine innate immune system: An update. *Dev. Comp. Immunol.* **45**, 321–343 (2014).
40. A. M. Antonson, E. C. Radlowski, M. A. Lawson, J. L. Rytch, R. W. Johnson, Maternal viral infection during pregnancy elicits anti-social behavior in neonatal piglet offspring independent of postnatal microglial cell activation. *Brain Behav. Immun.* **59**, 300–312 (2017).
41. A. M. Antonson, B. Balakrishnan, E. C. Radlowski, G. Petr, R. W. Johnson, Altered hippocampal gene expression and morphology in fetal piglets following maternal respiratory viral infection. *Dev. Neurosci.* **40**, 104–119 (2018).
42. M. M. McCarthy, Sex differences in neuroimmunity as an inherent risk factor. *Neuropsychopharmacology* **44**, 38–44 (2019).
43. S. E. Hickman *et al.*, The microglial sensome revealed by direct RNA sequencing. *Nat. Neurosci.* **16**, 1896–1905 (2013).
44. T. Town, V. Nikolic, J. Tan, The microglial “activation” continuum: From innate to adaptive responses. *J. Neuroinflammation* **2**, 24 (2005).
45. A. Nimmerjahn, F. Kirchhoff, F. Helmchen, Resting microglial cells are highly dynamic surveillants of brain parenchyma in vivo. *Science* **308**, 1314–1318 (2005).
46. D. Boche, V. H. Perry, J. A. Nicoll, Review: Activation patterns of microglia and their identification in the human brain. *Neuropathol. Appl. Neurobiol.* **39**, 3–18 (2013).
47. J. L. Bolton *et al.*, Gestational exposure to air pollution alters cortical volume, microglial morphology, and microglia-neuron interactions in a sex-specific manner. *Front. Synaptic Neurosci.* **9**, 10 (2017).
48. N. Swinnen *et al.*, Complex invasion pattern of the cerebral cortex by microglial cells during development of the mouse embryo. *Glia* **61**, 150–163 (2013).
49. C. Kozlowski, R. M. Weimer, An automated method to quantify microglia morphology and application to monitor activation state longitudinally in vivo. *PLoS One* **7**, e31814 (2012).
50. K. Ohsawa, Y. Imai, Y. Sasaki, S. Kohsaka, Microglia/macrophage-specific protein Iba1 binds to fimbrin and enhances its actin-bundling activity. *J. Neurochem.* **88**, 844–856 (2004).
51. P. Ji, K. M. Schachtschneider, L. B. Schook, F. R. Walker, R. W. Johnson, Peripheral viral infection induced microglial sensome genes and enhanced microglial cell activity in the hippocampus of neonatal piglets. *Brain Behav. Immun.* **54**, 243–251 (2016).
52. S. H. Fatemi *et al.*, The viral theory of schizophrenia revisited: Abnormal placental gene expression and structural changes with lack of evidence for H1N1 viral presence in placentae of infected mice or brains of exposed offspring. *Neuropharmacology* **62**, 1290–1298 (2012).
53. T. L. Tay, J. C. Savage, C. W. Hui, K. Bisht, M. E. Tremblay, Microglia across the lifespan: From origin to function in brain development, plasticity and cognition. *J. Physiol.* **595**, 1929–1945 (2017).
54. C. A. Mosser, S. Baptista, I. Arnoux, E. Audinat, Microglia in CNS development: Shaping the brain for the future. *Prog. Neurobiol.* **149–150**, 1–20 (2017).
55. J. M. Schwarz, S. D. Bilbo, Sex, glia, and development: Interactions in health and disease. *Horm. Behav.* **62**, 243–253 (2012).
56. R. Hanamsagar *et al.*, Generation of a microglial developmental index in mice and in humans reveals a sex difference in maturation and immune reactivity. *Glia* **65**, 1504–1520 (2017).
57. H. Stepanova, M. Mensikova, K. Chlebova, M. Faldyna, CD4+ and $\gamma\delta$ TCR+ T lymphocytes are sources of interleukin-17 in swine. *Cytokine* **58**, 152–157 (2012).
58. Y. H. Zhu *et al.*, Dose-dependent effects of *Lactobacillus rhamnosus* on serum interleukin-17 production and intestinal T-cell responses in pigs challenged with *Escherichia coli*. *Appl. Environ. Microbiol.* **80**, 1787–1798 (2014).
59. M. L. Estes, A. K. McAllister, Maternal immune activation: Implications for neuropsychiatric disorders. *Science* **353**, 772–777 (2016).
60. J. R. Groom, A. D. Luster, CXCR3 in T cell function. *Exp. Cell Res.* **317**, 620–631 (2011).
61. A. Urakubo, L. F. Jarskog, J. A. Lieberman, J. H. Gilmore, Prenatal exposure to maternal infection alters cytokine expression in the placenta, amniotic fluid, and fetal brain. *Schizophr. Res.* **47**, 27–36 (2001).
62. J. H. Gilmore, L. F. Jarskog, S. Vadlamudi, Maternal infection regulates BDNF and NGF expression in fetal and neonatal brain and maternal-fetal unit of the rat. *J. Neuroimmunol.* **138**, 49–55 (2003).
63. J. H. Gilmore, L. F. Jarskog, S. Vadlamudi, Maternal poly I:C exposure during pregnancy regulates TNF α , BDNF, and NGF expression in neonatal brain and the maternal-fetal unit of the rat. *J. Neuroimmunol.* **159**, 106–112 (2005).
64. C. N. Parkhurst *et al.*, Microglia promote learning-dependent synapse formation through brain-derived neurotrophic factor. *Cell* **155**, 1596–1609 (2013).
65. P. E. Batchelor *et al.*, Macrophages and microglia produce local trophic gradients that stimulate axonal sprouting toward but not beyond the wound edge. *Mol. Cell. Neurosci.* **21**, 436–453 (2002).
66. S. W. Lai *et al.*, Regulatory effects of neuroinflammatory responses through brain-derived neurotrophic factor signaling in microglial cells. *Mol. Neurobiol.* **55**, 7487–7499 (2018).
67. M. L. Bennett *et al.*, New tools for studying microglia in the mouse and human CNS. *Proc. Natl. Acad. Sci. U.S.A.* **113**, E1738–E1746 (2016).
68. G. W. Kreutzberg, Microglia: A sensor for pathological events in the CNS. *Trends Neurosci.* **19**, 312–318 (1996).
69. D. A. E. Hendrickx, C. G. van Eden, K. G. Schuurman, J. Hamann, I. Huitinga, Staining of HLA-DR, Iba1 and CD68 in human microglia reveals partially overlapping expression depending on cellular morphology and pathology. *J. Neuroimmunol.* **309**, 12–22 (2017).
70. M. R. Elmore *et al.*, Respiratory viral infection in neonatal piglets causes marked microglia activation in the hippocampus and deficits in spatial learning. *J. Neurosci.* **34**, 2120–2129 (2014).
71. X. Hu *et al.*, Microglial and macrophage polarization—New prospects for brain repair. *Nat. Rev. Neurol.* **11**, 56–64 (2015).
72. O. Butovsky *et al.*, Identification of a unique TGF- β -dependent molecular and functional signature in microglia. *Nat. Neurosci.* **17**, 131–143 (2014).
73. A. Buttgerieit *et al.*, Sall1 is a transcriptional regulator defining microglia identity and function. *Nat. Immunol.* **17**, 1397–1406 (2016).
74. S. Abutbul *et al.*, TGF- β signaling through SMAD2/3 induces the quiescent microglial phenotype within the CNS environment. *Glia* **60**, 1160–1171 (2012).
75. D. G. Walker, L. F. Lue, Immune phenotypes of microglia in human neurodegenerative disease: Challenges to detecting microglial polarization in human brains. *Alzheimers Res. Ther.* **7**, 56 (2015).
76. D. Mattei *et al.*, Maternal immune activation results in complex microglial transcriptome signature in the adult offspring that is reversed by minocycline treatment. *Transl. Psychiatry* **7**, e1120 (2017).
77. Y. Shigemoto-Mogami, K. Hoshikawa, J. E. Goldman, Y. Sekino, K. Sato, Microglia enhance neurogenesis and oligodendrogenesis in the early postnatal subventricular zone. *J. Neurosci.* **34**, 2231–2243 (2014).
78. B. Arnò *et al.*, Neural progenitor cells orchestrate microglia migration and positioning into the developing cortex. *Nat. Commun.* **5**, 5611 (2014).
79. M. Nakanishi *et al.*, Microglia-derived interleukin-6 and leukemia inhibitory factor promote astrocytic differentiation of neural stem/progenitor cells. *Eur. J. Neurosci.* **25**, 649–658 (2007).
80. C. Béchade, O. Pascual, A. Triller, A. Bessis, Nitric oxide regulates astrocyte maturation in the hippocampus: Involvement of NOS2. *Mol. Cell. Neurosci.* **46**, 762–769 (2011).
81. Y. Hattori, T. Miyata, Microglia extensively survey the developing cortex via the CXCL12/CXCR4 system to help neural progenitors to acquire differentiated properties. *Genes Cells* **23**, 915–922 (2018).
82. K. A. Garbett, E. Y. Hsiao, S. Kálmán, P. H. Patterson, K. Mirnics, Effects of maternal immune activation on gene expression patterns in the fetal brain. *Transl. Psychiatry* **2**, e98 (2012).
83. N. Wu *et al.*, alpha-Crystallin downregulates the expression of TNF-alpha and iNOS by activated rat retinal microglia in vitro and in vivo. *Ophthalmic Res.* **42**, 21–28 (2009).
84. J. E. Dulle, P. E. Fort, Crystallins and neuroinflammation: The glial side of the story. *Biochim. Biophys. Acta* **1860**, 278–286 (2016).
85. B. Pickard, Progress in defining the biological causes of schizophrenia. *Expert Rev. Mol. Med.* **13**, e25 (2011).
86. P. A. Spadaro *et al.*, Long noncoding RNA-directed epigenetic regulation of gene expression is associated with anxiety-like behavior in mice. *Biol. Psychiatry* **78**, 848–859 (2015).
87. K. Askew *et al.*, Coupled proliferation and apoptosis maintain the rapid turnover of microglia in the adult brain. *Cell Rep.* **18**, 391–405 (2017).
88. D. Nayak, B. H. Zinselmeyer, K. N. Corps, D. B. McGavern, In vivo dynamics of innate immune sentinels in the CNS. *Intravital* **1**, 95–106 (2012).
89. Q. Li, B. A. Barres, Microglia and macrophages in brain homeostasis and disease. *Nat. Rev. Immunol.* **18**, 225–242 (2018).
90. M. Zhou *et al.*, CCR5 is a suppressor for cortical plasticity and hippocampal learning and memory. *eLife* **5**, e20985 (2016).
91. A. Dityatev, D. A. Rusakov, Molecular signals of plasticity at the tetrapartite synapse. *Curr. Opin. Neurobiol.* **21**, 353–359 (2011).
92. A. R. Bialas, B. Stevens, TGF- β signaling regulates neuronal C1q expression and developmental synaptic refinement. *Nat. Neurosci.* **16**, 1773–1782 (2013).
93. I. D. Vainchtein *et al.*, Astrocyte-derived interleukin-33 promotes microglial synapse engulfment and neural circuit development. *Science* **359**, 1269–1273 (2018).
94. S. H. Chen *et al.*, Microglial regulation of immunological and neuroprotective functions of astroglia. *Glia* **63**, 118–131 (2015).

95. S. A. Liddelow *et al.*, Neurotoxic reactive astrocytes are induced by activated microglia. *Nature* **541**, 481–487 (2017).
96. H. G. Bernstein, Y. Piontkewitz, G. Keilhoff, Commentary: Maternal immune activation evoked by polyinosinic: Polycytidylic acid does not evoke microglial cell activation in the embryo. *Front. Cell. Neurosci.* **10**, 41 (2016).
97. D. Ibi, K. Yamada, Therapeutic targets for neurodevelopmental disorders emerging from animal models with perinatal immune activation. *Int. J. Mol. Sci.* **16**, 28218–28229 (2015).
98. U. Meyer *et al.*, The time of prenatal immune challenge determines the specificity of inflammation-mediated brain and behavioral pathology. *J. Neurosci.* **26**, 4752–4762 (2006).
99. K. Grabert *et al.*, Microglial brain region-dependent diversity and selective regional sensitivities to aging. *Nat. Neurosci.* **19**, 504–516 (2016).
100. W. C. Pierre *et al.*, Neonatal microglia: The cornerstone of brain fate. *Brain Behav. Immun.* **59**, 333–345 (2017).